# EUROPEAN ORGANIZATION FOR NUCLEAR RESEARCH

# Isotope Shift of $^{182}$Hg and an Update of Nuclear Moments and Charge Radii in the Isotope Range $^{181}$Hg - $^{206}$Hg

G. Ulm[1], S.K. Bhattacherjee[2], P. Dabkiewicz[3], G. Huber, H.-J. Kluge[1],

T. Kühl[4], H. Lochmann[5], E.-W. Otten, K. Wendt

Institut für Physik, Universität Mainz, Mainz, Fed. Rep. Germany

S.A. Ahmad[6], W. Klempt, R. Neugart[7]

and

The ISOLDE Collaboration

CERN, Geneva, Switzerland

[1] Present address: CERN, Geneva, Switzerland

[2] On leave from Tata Institute of Fundamental Research, Bombay, India

[3] Present address: Technische Universität, Hamburg-Harburg, FRG

[4] Present address: Gesellschaft für Schwerionenforschung, Darmstadt, FRG

[5] Present address: W.C. Heraeus GmbH, Hanau, FRG

[6] On leave from Bhabha Atomic Research Centre, Bombay, India

[7] Present address: Institut für Physik, Universität Mainz, FRG

Abstract:   The technique of collinear fast-beam laser spectroscopy has been
used to measure the isotope shifts of the even-even isotopes of Hg
(Z=80) in the mass range $182 \leq A \leq 198$ at the on-line mass separator
ISOLDE at CERN. The atomic transition studied (6s6p $^3P_2$ - 6s7s $^3S_1$, $\lambda$
= 546.1 nm) starts from a metastable state, which is populated in a
quasi resonant charge transfer process. The resulting changes in
nuclear mean square charge radii show clearly that $^{182}$Hg follows the
trend of the heavier, even, weakly oblate isotopes. Correspondingly the
huge odd-even shape staggering in the light Hg isotopes continues and
the nuclear shape staggering and shape coexistence persists down to
the last isotope investigated, $^{181}$Hg. An update of isotope shift and
hyperfine structure data for $^{181-206}$Hg is given, with a revised
evaluation of the differences in nuclear mean square charge radii and of
spectroscopic quadrupole moments.

1. Introduction

Systematic studies by optical spectroscopy on long isotopic chains are a
main source of information on nuclear ground state properties [1]. The
hyperfine structure (hfs) and isotope shift (IS) of optical spectra allow the
determination of the nuclear spins I, magnetic dipole moments $\mu$, spectro-
scopic quadrupole moments $Q_s$, and the changes of the nuclear mean square
charge radii $\delta \langle r^2 \rangle$.

The first element for which many isotopes were studied by optical methods
is Hg (Z = 80). This element is also exemplary for the interdependence of

the development of experimental techniques concerning sensitivity and resolution on the one hand and accessibility of the isotopes on the other. Conventional optical spectroscopy has yielded data in the isotope range $192 \leq A \leq 204$ [2], [3]. The method of $\gamma$ radiation detected optical pumping ($\gamma$-RADOP) was first developed to investigate the isotopes $^{203}$Hg [4] and $^{199m}$Hg [5]. Measurements by the $\beta$ radiation detected optical pumping method ($\beta$-RADOP) extended our knowledge of nuclear ground state properties for the odd Hg isotopes into the mass range $181 \leq A \leq 191$ and to $^{205}$Hg [6], [7], [8]. One of the striking features resulting from this experiment was the large change in the $\delta \langle r^2 \rangle$ value between the isotopes $^{187}$Hg and $^{185}$Hg, which was attributed to a sudden oblate-prolate shape transition [6]. Since the RADOP method is not applicable to I = 0 nuclei, a pulsed laser system was later used to measure the IS of the even Hg isotopes in the mass region $184 \leq A \leq 190$ and of $^{206}$Hg. In addition the hfs and IS of the I = 13/2 isomeric states of the odd isotopes, $185 \leq A \leq 191$, could be studied. Preliminary results of these experiments using pulsed lasers have been published earlier [9], [10], [11], [12]. This work reports IS measurements on even mass Hg isotopes in the range $182 \leq A \leq 198$ by collinear laser spectroscopy, which includes for the first time $^{182}$Hg (preliminarily reported at the Alushta Heavy Ion Meeting 1983 [13]). All the measurements on short-lived Hg isotopes were performed at the on-line mass separator ISOLDE at CERN, Geneva [14].

After a brief description of the experiment in Section 2, a compilation of IS data of Hg isotopes is given in Section 3, including the values resulting from the final evaluation of the data from the earlier pulsed-laser experiments. The interpretation and discussion in Section 4 concentrates on the nuclear charge radii and shapes of the Hg isotopes, throwing new light on

that interesting region. The re-evaluation of $\delta\langle r^2\rangle$ and $Q_s$ is based on new values for the electronic field shift factor and the electronic field gradient treated in two Appendices.

## 2. Experiment

As in previous experiments the neutron deficient Hg isotopes were produced at the ISOLDE facility at CERN [14] in a spallation reaction of 600 MeV protons on a molten-lead target. The volatile Hg fraction of the reaction products was ionized in a plasma ion source with a production yield as given in [14]. Special care was taken in the setting of the ion source in order to form an ion beam with constant energy and small emittance. The extracted 60 keV beam was mass separated and directed to the apparatus for collinear fast-beam laser spectroscopy.

Most of the known optical data on radioactive isotopes of Hg have been obtained in the ultraviolet intercombination line $6s^2$ $^1S_0$ - $6s6p$ $^3P_1$ ($\lambda$ = 253.7 nm). In spite of the deeply bound atomic ground states of $Hg^+$ and Hg the versatility of collinear laser spectroscopy, however, allowed the use of cw dye lasers in the visible range. The $Hg^+$ ions passed through a sodium vapour cell. Since the charge exchange process favours a resonant electron transfer, the metastable $6s6p$ $^3P_2$ state is strongly populated (see Fig. 1). This efficient mechanism for producing beams of metastable atoms was first exploited in collinear laser spectroscopy on hydrogen [15] and ytterbium [16].

The metastable Hg atoms were excited to the 6s7s $^3S_1$ state by a single mode dye laser at $\lambda$ = 546.1 nm. The resonance was detected by the 453.8 nm and 404.7 nm transitions to the 6s6p $^3P_1$ and $^3P_0$ states, respectively. Fluorescence photons were focussed by an ellipsoidal mirror onto a RCA 8850 photomultiplier, which was blocked from the 546.1 nm laser stray light by a colour filter. Details on the experimental set-up are given in [17] for the charge exchange and detection chamber and in [18] for the laser, beam handling, and data taking. Fig. 2 shows a set of resonances for some of the isotopes, obtained by Doppler-tuning of the absorption frequency of the fast-beam atoms at a fixed laser frequency.

## 3. Results

### 3.1 Isotope Shift and Differences in Nuclear Mean Square Charge Radii

The IS data evaluated from the observed resonances in the $\lambda$ = 546.1 nm transition for $^{182}$Hg to $^{196}$Hg are listed in Table 1 with $^{198}$Hg taken as a reference. Our result for $^{196}$Hg is in perfect agreement with the value reported from high resolution measurements on stable isotopes [19]. In addition, the weighted means of IS data measured in the $\lambda$ = 253.7 nm line including the final results of the pulsed laser experiment [20] are compiled. The isotope shift $\delta\nu_i^{A,A'}$ between two isotopes with mass A and A' in an optical transition i is the sum of the mass shift $\delta\nu_{MS,i}$ and the field shift $\delta\nu_{FS,i}$ (see, for example, [31] and [32])

$$\delta\nu_i^{A,A'} = \nu_i^{A'} - \nu_i^A = \delta\nu_{MS,i}^{A,A'} + \delta\nu_{FS,i}^{A,A'} \quad , \tag{1}$$

where the mass shift is the sum of the normal (NMS) and the specific mass shift (SMS)

$$\delta \nu_{M,i}^{A,A'} = (A'-A)/(A'A) \times \{M_{NMS,i} + M_{SMS,i}\} \quad . \tag{2}$$

The field shift is given by

$$\delta \nu_{FS,i}^{A,A'} = F_i \lambda^{A,A'} \tag{3}$$

where $F_i$ is the electronic factor and the nuclear parameter, $\lambda^{A,A'}$, is connected to the change of the nuclear mean square charge radii $\delta \langle r^2 \rangle$ via [33]

$$\lambda^{A,A'} = \delta \langle r^2 \rangle^{A,A'} + (C_2/C_1)\delta \langle r^4 \rangle^{A,A'} + (C_3/C_1)\delta \langle r^6 \rangle^{A,A'} + \ldots \quad . \tag{4}$$

Multi-configuration Dirac-Fock (MCDF) calculations by Torbohm et al. [34] resulted in coefficients $C_i$ which differ only slightly from the values tabulated by Seltzer [33] in use till now.

The evaluation of $\lambda^{A,A'}$ from the IS data compiled in Table 1 is based on the following values for the $\lambda = 253.7$ nm transition: (i) The specific mass shift $SMS_{254}$ is assumed to be $(0\pm0.5)NMS_{254}$ in accordance with the empirical estimates for ($ns^2$ - nsnp) transitions [31]. (ii) We use the electronic factor $F_{254}$ as given by an ab initio MCDF calculation [34] to be (see Appendix A)

$$F_{254} = -55.36 \text{ GHz/fm}^2 \tag{5}$$

for the isotope pair (198,204). The small dependence of $F_i$ on the mass number is taken into account by scaling (5) according to the expression given by Blundell et al. [35].

The IS values in the $\lambda$ = 546.1 nm transition are related to those in the 253.7 nm line by a King-plot [36] (Fig. 3), which gives a slope

$$\kappa = F_{546}/F_{254} = -0.1707(12) \tag{6}$$

and an intercept corresponding to a specific mass shift

$$SMS_{546} = 0.37(56) \times NMS_{546} \tag{7}$$

where assumption (i) above was used for $SMS_{254}$. Such a small SMS is in agreement with the usual estimates for the SMS.

The $\lambda^{A,A'}$ parameters deduced by this procedure from the IS data of the two lines are consistent within the experimental errors, with the exception of $^{182}$Hg and $^{199}$Hg (see Fig. 3).

Using the relation (4) the differences in the mean square charge radii $\delta\langle r^2 \rangle$ can be related to $\lambda$ by approximating the small contributions from higher radial moments with an expression derived from the usual two parameter model of the nuclear shape [37].

$$\lambda^{A,A'} - \delta\langle r^2 \rangle^{A,A'} = x\delta\langle r^2 \rangle_{sph}^{A,A'} + y[5/(4\pi)]\overline{\langle r^2 \rangle}_{sph}\delta\langle \beta_2{}^2 \rangle^{A,A'} , \tag{8}$$

where

$$x = 10C_2/(7C_1)\overline{R}^2 + 5C_3/(3C_1)\overline{R}^4 ,$$

$$y = 2C_2/C_1\overline{R}^2 + 3C_3/C_1\overline{R}^4 \text{ , and}$$
$$\overline{R} = 1.2 \ \overline{A}^{1/3} \text{ fm and } \overline{A} = (A+A')/2.$$

The values $\langle r^2 \rangle_{sph}$ and $\delta\langle r^2 \rangle_{sph}$ are taken from the droplet model [38]. $\delta\langle r^2 \rangle^{A,A'}$ was evaluated for a given $\lambda^{A,A'}$ in an iterative way starting with a preliminary calculation according to (4) with coefficients $C_i$ from [34] and decomposing this result into a spherical and a deformation part (see (12),(13)) used then in (8). The final results are presented in column 4 of Table 1.

## 3.2 Hyperfine Structure and Nuclear Moments

Hyperfine interaction constants of the 6s6p $^3P_1$ state of Hg I and nuclear moments were compiled by Bonn et al. [8] for the mass range $^{181-205}$Hg. This compilation included the data obtained by the RADOP technique for the ground states of $^{181-191}$Hg, $^{205}$Hg, and $^{199m}$Hg. Optical spectroscopy with pulsed lasers on atoms confined in a resonance cell has been applied to the ground and isomeric states of neutron deficient isotopes in the mass range $^{185-191}$Hg. The results for the I=13/2 isomers $^{185m-191m}$Hg were published by Dabkiewicz et al. [12]. The resulting hfs parameters and deduced nuclear magnetic dipole moments for the ground states of $^{185-191}$Hg are listed in Table 2 together with the final results for $^{185m}$Hg [20].

The spectroscopic quadrupole moments (corrected for the Sternheimer effect, see Table 3) are extracted from the measured B factors by relating them to the quadrupole moment of the stable isotope $^{201}$Hg by

$$^{A}Q_{s} = \,^{201}Q_{s} \times \,^{A}B/^{201}B \quad . \qquad\qquad (9)$$

For that purpose $^{201}Q_{s}$ has been recalculated on the basis of a re-evaluation of the electric hfs field of the precisely measured quadrupole splitting of the 6s6p $^{3}P_{2}$ state [39] which is given by

$$B(^{3}P_{2}) = \,^{3}b_{P_{3/2}} = (2/5)(e^{2}/h)\,Q_{s}\,^{3}\langle r^{-3}\rangle_{p}\,R_{P_{3/2}}(Z_{i})\,(1-R)\ . \qquad (10)$$

The essential radial parameter $^{3}\langle r^{-3}\rangle_{p}$ as well as the relativistic $R_{P_{3/2}}(Z_{i})$ and Sternheimer correction factors $(1-R)$ are discussed in Appendix B. The new result is

$$^{201}Q_{s} = 0.372(40)\ b \qquad\qquad (11)$$

which is used in (9) to calculate the $Q_{s}$ values given in Table 3.

It agrees well with the result $^{201}Q_{s} = 0.386(49)$ b obtained recently from the muonic 3d-2p transition in $^{201}Hg$ [41]. (The 2p-1s muonic transition yielded a much smaller value due to nuclear polarization.) Furthermore good agreement is found with $^{201}Q_{s} = 0.39(2)$ b which was deduced from a time-dependent directional correlation study in combination with results from a nuclear quadrupole resonance experiment [42].

## 4. Interpretation and Discussion

### 4.1 Changes in Mean Square Charge Radii

The change in the nuclear mean square charge radii, $\delta\langle r^2\rangle$, relative to $^{198}$Hg, is plotted in Fig. 4 versus the mass number for the whole Hg isotopic chain. The regular and smooth variation of $\delta\langle r^2\rangle$ in the heavier isotopes continues in $^{186}$Hg, $^{185m}$Hg, $^{184}$Hg and $^{182}$Hg. The most outstanding features of the data are the following:

(i)     A strong discontinuity occurs for the light odd isotopes with A<186,

(ii)    The exceptionally large isomer shift in $^{185}$Hg, which is surpassed only by those of the fission isomers, and finally

(iii)   The odd-even staggering in the $\delta\langle r^2\rangle$-values of the lighter Hg nuclei is the largest ever observed.

When the sudden change in the charge radii between $^{187}$Hg and $^{185}$Hg was discovered in 1972 [6], its interpretation as a deformation effect was doubted, because the proton shell is almost closed. Instead of this, a change of the monopole charge distribution was advocated [43]. This idea has been taken up again in a very recent calculation [44]. However, much evidence has been gathered experimentally and theoretically favouring the interpretation in terms of collective $\beta_2$ deformation (reviewed in [8] and more recently in [45], [46]). Now it is widely accepted that the light even Hg isotopes, as well as $^{185m}$Hg, and those with A≥186 have a small oblate

deformation, while the light odd isotopes $^{181}$Hg, $^{183}$Hg, and $^{185}$Hg are strongly deformed and prolate. Hence, the odd-even staggering in light Hg isotopes is due to nuclear shape transitions, and the large isomer shift is the clearest demonstration for shape coexistence. The sharpness of the shape transitions is caused by the reinforcement of proton and neutron shell gaps due to the competing shells (almost magic proton number Z = 80, midshell neutron number N = 104).

Supplemental information on the shape transition and coexistence in the Hg region has been obtained by nuclear spectroscopy. Here, competing near-spherical and deformed bands have been discovered. Furthermore, high angular momentum intruder states have been identified which induce deformation [45], [46].

Before resuming this discussion with respect to the case of $^{182}$Hg and related questions we shall present an evaluation of deformation parameters from $\delta\langle r^2 \rangle$.

## 4.2 Relationship between $\delta\langle r^2 \rangle$ and Deformation

The $\delta\langle r^2 \rangle$ data obtained by optical spectroscopy are model independent except for the small corrections for higher orders in $\lambda^{A,A'}$ (see Eq. (4),(8)). The following interpretation of $\delta\langle r^2 \rangle$, however, is model dependent and based on the usual two parameter model assuming a decomposition of $\delta\langle r^2 \rangle$ into a spherical part describing the change in nuclear volume and into a deformation part at constant volume

$$\delta\langle r^2 \rangle^{A,A'} = \delta\langle r^2 \rangle_{sph}^{A,A'} + \delta\langle r^2 \rangle_{def}^{A,A'} \quad . \tag{12}$$

This model was used already in our earlier papers on Hg [8], [9], [10], [11], [12], but we have to point at two differences in the present analysis:

(i) The $\delta\langle r^2\rangle$ scale has changed from $1/F = 0.0223(20)$ fm²/GHz to $1/F = 0.0181(13)$ fm²/GHz, i.e. to a 20 % smaller variation of $\delta\langle r^2\rangle$ (see Appendix A).

(ii) At the time of our earlier publications there was no generally accepted model in use to describe the A dependence of the volume part $\delta\langle r^2\rangle_{sph}$. Therefore this dependence was adjusted locally and, more or less, empirically to the data [8]. In the meantime a large number of new IS data has been collected over extended regions of the nuclear chart. Except for some local difficulties (which could be a matter of choosing incorrect F-values) these data seem to be generally consistent with the droplet model [38], which describes the mean square charge radii of spherical nuclei as a function of N and Z. Therefore it is used also here to calculate the first term in (12). Recently, an increase of the droplet slope was proposed [47], [48], which, however, affects the deformation parameters deduced via (12),(13) within the Hg chain only slightly (see below). The deformation contribution is given by

$$\delta\langle r^2\rangle_{def}^{A,A'} = [5/(4\pi)]\langle r^2\rangle_{sph}[\delta\langle\beta_2^2\rangle^{A,A'} + \delta\langle\beta_3^2\rangle^{A,A'} + \delta\langle\beta_4^2\rangle^{A,A'}] \, ,$$
(13)

where quadrupole, octupole and hexadecapole deformation are considered. Usually the change in static or dynamic quadrupole deformation $\beta_2$ is the dominant contribution to $\delta\langle r^2\rangle_{def}$ and the data are well described by con-

sideration of only $\delta\langle\beta_2^2\rangle$.    Changes of $\langle\beta_2^2\rangle$ along an isotopic chain can then be determined relative to a reference isotope.    Absolute values of $\langle\beta_2^2\rangle$ can be evaluated if $\langle\beta_2^2\rangle$ is known for at least one isotope.  For the even isotopes $\langle\beta_2^2\rangle$ can be taken from the reduced transition probabilities B(E2) through a closure relation

$$\langle\beta_2^2\rangle = \Sigma_i \, (4\pi/3ZR_0^2)^2 \, B(E2, \, 0^+ \rightarrow 2_i^+) \, , \qquad (14)$$

with $R_0 = 1.2 \, A^{1/3}$ fm.  The sum in (14) reduces essentially to the first term [49].   The root mean square deformation, $\langle\beta_2^2\rangle^{1/2}$, calculated approximately from known B(E2, $0^+ \rightarrow 2_1^+$) values, is listed in column 6 of Table 1.   Assuming $\langle\beta_2^2\rangle^{1/2} = 0.106$ for $^{198}$Hg as a calibration and neglecting changes in $\langle\beta_3^2\rangle$ and $\langle\beta_4^2\rangle$ the deformation parameters of all the Hg isotopes are calculated via (12) and (13) and listed in column 5 of Table 1.

## 4.3 Deformation of Heavier Hg Isotopes

The agreement between $\langle\beta_2^2\rangle^{1/2}$ determined from B(E2)-values and from the IS data assuming only changes in the quadrupole deformation is satisfactory. The only exceptions are the deformation parameters in the range from $^{202}$Hg to $^{206}$Hg, where decreasing $\langle\beta_2^2\rangle^{1/2}$ from the B(E2) values are consistent with an expected decrease of quadrupole deformation towards the neutron shell closure at N = 126. In contrast to this behaviour the isotope shifts indicate a roughly constant deformation of $\langle\beta_2^2\rangle^{1/2} \cong 0.10$ (neglecting higher order deformation). $\beta_2$ deduced from IS data would change to 0.06 for $^{206}$Hg, e.g., by a proposed 15 % increase of the droplet slope

[47], [48], [56], reducing the disagreement with the deformation parameters from B(E2) values in this mass region. Various other reasons might cause the discrepancy:

(i) Because of the lack of data, the sum in (14) has been truncated to the first term in calculating $\langle\beta_2{}^2\rangle$. This may be unjustified near the shell closure.

(ii) The droplet model used to describe the change in nuclear volume within an isotopic chain is a macroscopic model which is not expected to reproduce structure in $\delta\langle r^2\rangle_{sph}$ due to shell or subshell closures. Evidence for a subshell closure can be seen at $N = 120$ in the two-neutron separation energies $S(2n)$ of Hg as tabulated by Wapstra and Audi [57] and in a differential plot of the IS data, $\delta\langle r^2\rangle^{N-2,N}$ (Fig. 5). For the neighbouring element Pb ($Z=82$) neither the $S(2n)$ values nor $\delta\langle r^2\rangle^{N-2,N}$ give an indication for such a pronounced subshell effect at this neutron number. In fact, the overall variation of $\delta\langle r^2\rangle^{208,A}$ of the lead isotopes with $N < 126$ is in good agreement with the predictions of the spherical droplet model [58], [59].

(iii) $\langle\beta_2{}^2\rangle_{IS}{}^{1/2}$ has been derived by the simple model, in which shape effects with the exception of quadrupole deformation have been neglected. Andl et al. [60] discussed ground state correlations due to octupole vibrations and their influence on the variation of the charge radii of Ca isotopes. A deformation parameter $\beta_3 = 0.076$ for $^{204}$Hg has been deduced by Baxter et al. [61] from an $\alpha$-scattering experiment. Using this $\beta_3$ value in (13) one obtains agreement for the case of $^{204}$Hg. This implies a change of $\langle\beta_3{}^2\rangle$ to zero towards $^{188}$Hg. Unfortunately no $\beta_3$ values for other mercury isotopes have been measured. Recent multiple Coulomb excitation measurements on $^{202,204}$Hg [62] have shown that the collectivity in the neutron rich Hg nuclei is of more complex origin than expected from the

few proton and neutron holes with respect to the $Z = 82$ and $N = 126$ major shells.

(iv) The influence of the variation of $\beta_4$ can be estimated from the calculation of Möller and Nix [63]: It gives only a small additional uncertainty to $\langle\beta_2{}^2\rangle^{1/2}$ since $|\beta_4|$ is predicted to vary only between 0 and 0.035 in the range from $^{206}$Hg to $^{182}$Hg.

(v) A decrease of the intrinsic skin diffuseness towards major shell closures might significantly contribute to $\delta\langle r^2\rangle$ not accounted for by (13). Such an effect was suggested to explain the IS data of Kr [64]. In Hg it would increase the observed discrepancy, however.

## 4.4 The Region of Shape Staggering

As has been mentioned above, the onset of strong deformation in the light even-A Hg isotopes was the subject of many theoretical papers [43], [65], [66], [67], [68]. These calculations differ in the prediction of the mass number at which the shape transition should occur, but they all expect the ground state of $^{182}$Hg to be strongly prolate. In contrast to this the calculation of Frauendorf and Pashkevich [69] predicts small oblate deformations for the ground states of all the even-mass isotopes including $^{182}$Hg. Bengtsson et al. [70] show potential-energy curves from the calculation of Möller and Nix [71] confirming this feature.

The IS measurement of $^{182}$Hg reported here has clearly decided this controversy in favour of the latter prediction. Independently, this was also concluded by Ma et al. [72] who established the level scheme of $^{182}$Hg for

the first time. They found the nuclear ground state to be the $0^+$ band head of an almost spherical band.

Concerning the odd-A isotopes, the calculations of Frauendorf and Pashkevich [69] showed that $^{181,183,185}$Hg should have a large prolate equilibrium deformation, whereas $^{187,189,191}$Hg have a small deformation, in agreement with the experiment. In their picture the shape transition is fostered by the prolate polarizing power of the [521 1/2] orbital coupled to the even core, and by its blocking effect. Below $^{186}$Hg the prolate shape gains about 0.5 MeV in binding energy relative to the oblate one [69], [73], which is, however, not reproduced by a recent Hartree-Fock calculation [74].

We finally note that our re-evaluation of IS changes the deduced deformation parameters of the light isotopes only slightly. For $^{181}$Hg, e.g., the value of $\langle \beta^2 \rangle^{1/2}$ = 0.32 published earlier [8] has now been changed to 0.28. An increase of the droplet slope by 15 % as mentioned above would change this value to 0.30.

4.5 Differential Isotope Shift and Odd-Even Staggering

Fig. 5 shows the differential changes of the charge radii upon addition of two neutrons, which accents the smaller changes in the trend of $\delta\langle r^2 \rangle$. A discontinuity is observed for Hg around N = 120, but not reproduced in Pb. The step at N = 104, the middle of the shell, indicates a change of

the deformation trend starting below $^{184}$Hg. Recently the Interacting Boson Model has been applied to a systematic study of the even Hg isotopes [75], [76], [77]. Apart from explaining various nuclear spectroscopic properties, it describes the IS data rather quantitatively. By fitting three parameters in the range $^{192-202}$Hg to the experimental values $\delta\langle r^2\rangle^{N-2,N}$ it reproduces an increasing value of $\delta\langle r^2\rangle^{N-2,N}$ in the middle of the neutron shell.

The odd-even staggering parameter $\gamma$, introduced by Tomlinson and Stroke [2] compares the change in the nuclear charge radii upon addition of one unpaired neutron to the effect of adding a neutron pair

$$\gamma^A = 2\delta\langle r^2\rangle^{A-1,A}/\delta\langle r^2\rangle^{A-1,A+1}; \quad A \text{ odd} \quad . \tag{15}$$

Fig. 6 shows the odd-even staggering of the Hg isotopes. The huge staggering parameters $\gamma^{183} = 11.2(5)$ and $\gamma^{185} = 13.6(5)$ interpreted as nuclear shape transitions are not included. Disregarding also $^{199m}$Hg, the normal situation is found where $\gamma$ is in the range $\gamma = 0$ to 1. Smooth trends, especially in the I = 13/2 isomers, are observed. A conspicuous trend of the odd-even staggering is also seen in the Pb isotopes [59].

Various theoretical approaches to describe the odd-even staggering effect [2], [78], [79] could not give a satisfactory explanation. Recently Talmi [80] succeeded in describing the staggering in the calcium isotopes by assuming different polarization of the core by a paired or an unpaired neutron. Zawischa [81] has suggested that four-particle correlations lead to staggering.

It can be hoped that the rich information available in the Hg isotopic chain, and especially that of the I = 13/2 isomers which have an almost pure con-figuration, will lead to a deeper quantitative understanding of the odd-even staggering effect.

## 4.6 Nuclear Moments

The measured nuclear magnetic dipole moments have been widely discussed in the literature, particularely by Bonn et al. [8] and by Ekström et al. [82], [83]. The striking feature of these experimental results is that far from the closed shell the magnetic moments of the I = 1/2, 3/2 and 13/2 states remain rather constant around 0.5 n.m., -0.6 n.m., and -1.0 n.m., respectively, over a wide range of neutron numbers. Even the strongly deformed light nuclei, $^{181,183,185}$Hg with I = 1/2, described by the Nilsson orbit [521 1/2], have moments very similar to those of the near-spherical heavier I = 1/2 ground states in $^{195,197,199}$Hg.

Tomlinson and Stroke [2] tried to explain the apparent constancy of the magnetic moments in the context of the independent-particle model. Re-cently the magnetic moments of the I = 13/2 isomers were calculated by Ragnarsson [73] and by Volmyanskii and Dubro [84] in a Particle-plus-Ro-tor model yielding good agreement with the experimental results.

The deformation parameter $\langle\beta_2\rangle$ can be obtained from the measured spectro-scopic quadrupole moments $Q_s$ in case of strong coupling by the projection formula

$$Q_0 = Q_s(I+1)(2I+3)/[I(2I-1)] \tag{16}$$

and the well-known relation [85]

$$Q_0 = [3/(5\pi)^{1/2}]ZR_0{}^2\langle\beta_2\rangle(1 + 0.36\langle\beta_2\rangle+\ldots) \qquad (17)$$

with $R_0 = 1.2\ A^{1/3}$ fm.

Application of (16),(17) yields for the I=3/2 ground-states of $^{187-193}$Hg a value of $\langle\beta_2\rangle\cong-0.13$, in remarkable agreement with $\langle\beta_2{}^2\rangle^{1/2}$ deduced from the IS data (see Table 1). This indicates that any dynamical effect entering into $\langle\beta_2{}^2\rangle^{1/2}$, but not in $\langle\beta_2\rangle$, is small. The negative $Q_s$ values are in agreement with many theoretical expectations [65], [67], [68]. Hence the strong-coupling scheme seems to be quite adequate for the ground states of these I = 3/2 nuclei, although the deformation is small.

On the other hand, for the I = 13/2 isomers, the strong-coupling projection formula fails completely; neither the sign nor the deformation parameters are reproduced [12]. The oblateness of the I = 13/2 isomers is in agreement with experimental findings like the decoupled band structure [86]. All these states appear to have nearly the same deformation (Table 1). Quantitative calculations for these isomeric $Q_s$ values by Ragnarsson [73] show excellent agreement with experimental values for a negative deformation parameter $\beta_2\cong-0.13$ (see also [83]). The theoretical variation of $Q_s$ clearly demonstrates the transition from strongly coupled high $\Omega$- to decoupled low $\Omega$-orbitals when the $i_{13/2}$ neutron shell is filled. This has been measured here for the first time in a sequence of isotopes, as pointed out by Faessler [87].

## 5. Conclusion

The isotope shift of $^{182}$Hg continues the steady trend of all even isotopes down from the neutron shell closure at $^{206}$Hg; it is compatible with a regular contraction of nuclear volume according to the droplet model, accompanied by small deformation. On the other hand, it establishes once more the phenomenon of odd-even shape staggering which so far is unique in the light Hg isotopes. The re-evaluated quadrupole moments and $\delta\langle r^2\rangle$ values are generally in good agreement with those derived from nuclear spectroscopy. Near the shell closure, however, the collective contribution to $\langle r^2\rangle$ is stronger than calculated on the basis of B(E2) values alone.

Concerning the experimental side it seems interesting to continue the measurements in the shape staggering region, and to search in particular for deformed odd isomers with I > 1/2, in order to confirm the magnitude and sign of the static deformation by a spectroscopic quadrupole moment.

## 6. Acknowledgement

Appendix A

The Electronic Field Shift Factor for the Transition $6s^2\ {}^1S_0$ - $6s6p\ {}^3P_1$ ($\lambda$ = 253.7 nm) of Hg I.

The electronic field shift factor $F_i$ of an optical transition i can be determined in the following ways:

(i) By ab initio calculations such as the Dirac-Fock (DF) or the multi-configuration Dirac-Fock (MCDF) method (see [34] and references therein).

(ii) By the widely-used semi-empirical method described for example by Heilig and Steudel [31].

(iii) By combining optical IS data with IS values from electronic or muonic X-ray spectra or results from electron scattering.

Bonn et al. [8] used a semi-empirical electronic field shift factor $F_{254}$ = -44.9(5.0) GHz/fm² for the transition $6s^2\ {}^1S_0$ - $6s6p\ {}^3P_1$ ($\lambda$ = 253.7 nm) of Hg I in accordance with [31]. This has been applied also to later results (e.g. [8], [10], [12]). Since this value of F is the only exception from an overall trend, namely, that the semi-empirical evaluation gives larger values than the ab initio theory [34], and since strong deviations from results determined by method (iii) are found, we give a revised evaluation of $F_{254}$ in the following. It is based on the results from recent experimental and theoretical work.

Recently Torbohm et al. [34] calculated electronic factors for various transitions in Hg I and Hg II in an ab initio approach. A DF calculation for the alkali-like transition $6s\ {}^2S_{1/2}$ - $6p\ {}^2P_{1/2}$ ($\lambda$ = 194.2 nm) in Hg II yields $F_{194}$ = -67.67 GHz/fm². The result of a MCDF calculation for the transition of interest in Hg I ($\lambda$ = 253.7 nm) is $F_{254}$ = -55.36 GHz/fm². The ratio $\kappa$

= $F_{254}/F_{194}$ = 0.818 can be compared with the slope of a King-plot (see below).

Following the conventions of Heilig and Steudel [31] the semi-empirical procedure is as follows: $F_i$ is factorized in an electronic factor $E_i$ depending on the change of the total non-relativistic electron charge density at the nucleus $\Delta|\Psi(0)|^2_i$ in an optical transition i and a relativistic correction factor $f(Z)$

$$F_i = E_i f(Z) = (\pi a_0^3/Z)\Delta|\Psi(0)|^2_i f(Z) \quad . \tag{A1}$$

$f(Z)$ is determined by the theoretical IS constant $C_{unif}$, which has recently been re-evaluated by Blundell et al. [35].

In the Hg I ($6s^2$ - $6s6p$) transition the problem of evaluating $\Delta|\Psi(0)|^2_{254}$ is shifted to the determination of the electron density of a 6s electron in the 6s $^2S_{1/2}$ ground state of Hg II via a King-plot of the 254 nm transition against the Hg II (6s - 6p, $\lambda$ = 194.2 nm) transition by

$$\Delta|\Psi(0)|^2_{254} = \kappa\Delta|\Psi(0)|^2_{194} = \kappa\beta|\Psi(0)|^2_{6s} = \gamma|\Psi(0)|^2_{6s} \quad , \tag{A2}$$

where $\beta$ and $\gamma$ are the usual screening factors. The DF calculation [34] gives $\beta$ = 1.038 and includes the relativistic $p_{1/2}$ contribution to $\Delta|\Psi(0)|^2_{194}$. The product $\gamma = \kappa\beta$ from the DF calculation, $\gamma$ = 0.849, is not in agreement with the result $\gamma$ = 0.743 of a non relativistic Hartree-Fock calculation by Wilson [88] and deviates from the value $\gamma$ = 0.67 used by Bonn et al. [8].

The 254/194 - King-plot yields the slope $\kappa$ = $F_{254}/F_{194}$ = 0.79(3) and an intersection of -4.9(4.3)$10^3$ GHz. ($IS_{194}$-data from [89]. ) Within the

large error the value of the intersection is compatible with the usual estimates [31] of the specific mass effect for (ns - np) and (ns² - nsnp) transitions. Since the King-plot introduces a strong correlation between the field shift and the mass shift and since the uncertainty of the intersection is so large we fix the specific mass shifts to the usual estimates. With this constraint $\kappa$ changes to 0.82(1) which is in excellent agreement with the result of the DF calculations.

The semi-empirical value of $|\psi(0)|^2_{6s}$ of Hg II can be determined by two widely used methods (see, for example Kopfermann [90]):

(i) The Goudsmit-Fermi-Segrè formula yields

$$|\psi(0)|^2_{6s} = Z_i Z_a^2/[\pi a_0^3(n-\sigma)^3](1-d\sigma/dn) = 26.75 \ a_0^{-3} \qquad \text{(A3)}$$

with $Z_i = Z = 80$, $Z_a = 2$, $(n-\sigma) = 1.7034$, $(1-d\sigma/dn) = 1.298$ (This value based on formula (26.33) in Kopfermann [90] results from a second order polynomial expression for the quantum defect $\sigma$, whereas Kopfermann used a linear variation of $\sigma$ with the term value, giving $(1-d\sigma/dn) = 1.248$).

(ii) From the hyperfine splitting of the 6s $^2S_{1/2}$ ground state of $^{199}$Hg II one obtains

$$|\psi(0)|^2_{6s} = 3\times1836.12 a_{6s}/[8\pi a_0^3\alpha^2 Ry \times g_I F_r(Z)(1-\delta)(1-\varepsilon)] = 25.43 \ a_0^{-3} \qquad \text{(A4)}$$

with $a_{6s} = 1351.17969$ mK [91], $g_I = 1.011770(2)$ [92], the relativistic correction factor $F_r(80) = 2.2573$ [90], the Breit-Rosenthal correction $(1-\delta) = 0.901$ [93], and the Bohr-Weisskopf correction $(1-\varepsilon) = 0.968$ [93].

Both semi-empirical values agree within 5%. The mean of (A3) and (A4) is inserted into (A1) via (A2) with $\beta = 1.038$ and $\kappa = 0.82$. The final result of the semi-empirical approach is

$$F_{254} = -60.3 \text{ GHz/fm}^2 \hspace{3cm} \text{(A5)}$$

for the isotope pair $^{204}$Hg and $^{198}$Hg with an estimated uncertainty of 10%.

Table A1 shows a comparison of results derived by the different methods including the experimental values from electronic and muonic X-rays. Some remarks should be made:

(i) The semi-empirical $F_i$ value is larger than the ab initio one, which is the usual trend.

(ii) All the results agree within roughly ±7%.

(iii) A correction of -12% for the spin exchange core polarization to the hfs has been applied in Cd II by Bauche et al. [95]. Such a correction would lower the value of $F_{254}$ as obtained by (A4). Other problems associated with the semi-empirical procedure are discussed by Bauche [96], by Blundell et al. [97], and by Torbohm et al. [34].

In conclusion we choose the result of the ab initio MCDF calculation with an assumed uncertainty in $F_{254}$ of 7%, which covers the results determined by all other methods. The electronic factor determined in the analysis of King [32], essentially based on the X-ray data, is slightly lower but in agreement with our choice within the limits of error.

Appendix B

RECALCULATION OF THE ELECTRIC HYPERFINE FIELD

$^{201}Q_s$ = 0.455(40) b was used in [5], [7], [8], [12] for the evaluation of the spectroscopic quadrupole moments of the unstable isotopes measured. This value which was obtained by McDermott and Lichten [39] via the unmodified Breit-Wills theory ($\lambda_p$ = 1, see below) includes corrections as given by Murakawa [98] who revised his analysis later [99]. Various other authors have used the unmodified Breit-Wills theory for the analysis of the 6s6p $^{2S+1}P_J$ configuration. References and results for $^{201}Q_s$ are compiled in Table VI of [27]. In the following a re-evaluation of $^{201}Q_s$ is given which is partly based on the modified Breit-Wills theory.

The HFS splitting of a nsnp $^{2S+1}P_J$ configuration is treated in [90], [100], [101]. The B factor of the 6s6p $^3P_2$ state is equal to the single-electron b factor, $^3b_{P_{3/2}}$, as given by (10). The superscript "3" indicates that the radial matrix element $^3\langle r^{-3}\rangle_p$ in (10) has to be taken for a radial p-wave function in a pure triplet state which differs from the one in the singlet state. In the frame of the modified Breit-Wills theory of the 6s6p configuration in Hg [100], [101] one obtains for the $\langle r^{-3}\rangle$ ratio in the singlet and the triplet states

$$^1\langle r^{-3}\rangle_p / {}^3\langle r^{-3}\rangle_p = \lambda_p{}^2 = 0.556 \ . \qquad \text{(B1)}$$

We evaluate $^3\langle r^{-3}\rangle_p$ semi-empirically by relating it (i) to the spin-orbit interaction, $\delta v_{so}$, and (ii) to the magnetic hfs interaction constant $^3a_{P_{3/2}}$.

$\langle r^{-3} \rangle$ CALCULATED FROM THE FINE STRUCTURE SPLITTING: Following Ref. [90] we can eliminate $^3\langle r^{-3} \rangle_p$ in (10) with the help of the Landé formula and obtain the moment $Q_{s,uncorr}$ uncorrected for the Sternheimer effect by

$$Q_{s,uncorr} = [(15\mu_B^2)/(2e^2)][(Z_i H_p(Z_i)/R_{P_{3/2}}(Z_i)][^3b_{P_{3/2}}/\delta v_{so}] . \quad (B2)$$

The second factor in (B2) contains the ratio of the relativistic corrections for spin-orbit and quadrupole interaction and amounts to 77.6 according to Schwartz's calculation [102]. The inner charge $Z_i$ is chosen as $Z - 4 = 76$. According to Ref. [103] $\delta v_{so}$ is obtained from the fine structure splitting $\delta v_{fs} = 1.918 \times 10^{14}$ Hz by applying a Z-dependent factor of 1.0585 which corrects for the contribution of spin-spin and spin-other-orbit interaction. Using these values and $^3b_{P_{3/2}} = B(^3P_2) = 399.150(2)$ MHz [39] one obtains

$$Q_{s,uncorr}(^{201}Hg) = 0.426 \text{ b} \quad (B3)$$

from an analysis of the fine structure splitting of Hg with the help of (B2).

$\langle r^{-3} \rangle$ CALCULATED FROM THE MAGNETIC HFS: Since the $^3\langle r^{-3} \rangle_p$ radial matrix element enters the single-electron interaction constants $^3a_{P_{3/2}}$ as well as $^3b_{P_{3/2}}$, the $\langle r^{-3} \rangle_p$ matrix element can be eliminated from the expression for the spectroscopic quadrupole moment (uncorrected for the Sternheimer effect) by

$$Q_{s,uncorr} = [8\mu_B\mu_n/(3e^2)][F_{3/2}(Z_i)/R_{P_{3/2}}(Z_i)][g_I {}^3b_{P_{3/2}}/{}^3a_{P_{3/2}}] . \quad (B4)$$

The second factor of (B4) contains the ratio of the relativistic correction factors $F_{3/2}(Z_i=76)/R_{P_{1/2}}(Z_i=76) = 0.889$ as given by Schwartz [102]. In order to calculate the ratio $^3b_{P_{3/2}}/^3a_{P_{3/2}}$ the single-electron interaction constant $^3a_{P_{3/2}}$ has to be extracted from the A factors in the different states of the (s,p)-configuration. It has been shown [104] that the contribution of the s electron cancels in the sum

$$S = A(^1P_1) + A(^3P_1) - A(^3P_2) \tag{B5}$$

which is equal to -812(7) MHz for $^{201}$Hg [105]. Using the effective operator parametrization of the (s,p)-hfs interaction given in [106], one easily verifies that also the core-polarization terms cancel in (B5). The sum reduces to

$$S = {}^1a^P_{01} + 3/5\ {}^3a^P_{12} = \lambda^2_p\ {}^3a^P_{01} + 3/5\ {}^3a^P_{12}\ . \tag{B6}$$

Remaining are the orbital and spin-dipolar interaction constants, the only ones whose radial matrix elements can be used in (10). The ratio of the magnetic interaction constants is given by

$$a^P_{01}/a^P_{12} = (2 + \gamma/5)/(\gamma - 2) \tag{B7}$$

with

$$\gamma = a_{P_{1/2}}/a_{P_{3/2}} = 5(1 - \delta_{P_{1/2}})(1 - \varepsilon_{P_{1/2}})\ \Theta(Z_i)\ . \tag{B8}$$

Eq. (B7) is derived from the effective operator parametrization of one-electron $a_{lj}$ factors [107] where the core-polarization term has been subtracted from the $a_{lj}$. The ratio $\gamma$ of these "bare" $a_{lj}$ is given predominantly by the

ratio of relativistic corrections $\Theta(Z_i=76) = 2.25$ [102]. Furthermore, it depends weakly on the Breit-Crawford-Schawlow correction, $\delta_{P_{1/2}} = 0.024$, and on the Bohr-Weisskopf effect which is estimated to give $\varepsilon = 0.008$ [90]. These latter corrections are negligable for $j = 3/2$. With (B5) - (B8) one calculates for $^{201}$Hg

$$^3a_{P_{3/2}} = -170(2) \text{ MHz} \quad . \tag{B9}$$

Using this value one obtains

$$Q_{s,uncorr}(^{201}\text{Hg}) = 0.422 \text{ b} \quad . \tag{B10}$$

The perfect agreement between (B3) and (B10) seems somewhat fortuitous in view of a discrepancy of up to 20 % found in a similar analysis of other group II elements [108].

For Hg no explicit calculation of the Sternheimer correction is available. Based on the systematics of calculations in similar spectra, Sternheimer estimates $(1 - R) = 1.14(4)$ [109]. Applying this correction we obtain

$$^{201}Q_s = 0.372(40) \text{ b} \tag{B11}$$

where the error is an estimate of systematic deficiencies of the formulas used.

References

[1]     Otten, E.W.: Nucl. Phys. A 354, 471c (1981)

[2]     Tomlinson, W.J., Stroke, H.H.: Nucl. Phys. 60, 614 (1964)

[3]     Davis, S.P., Aung, T., Kleinman, H.: Phys. Rev. 147, 861 (1966)

[4]     Cappeler, U., Mazurkewitz, W.: Journal of Magnetic Resonance 10, 15 (1973)

[5]     Bonn, J., Huber, G., Kluge, H.-J., Otten, E.W., Lode, D.: Z. Phys. A 272, 375 (1975)

[6]     Bonn, J., Huber, G., Kluge, H.-J., Kugler, L., Otten, E.W.: Phys. Lett. 38B, 308 (1972)

[7]     Huber, G., Bonn, J., Kluge, H.-J., Otten, E.-W.: Z. Phys. A 276, 187 (1976)

[8]     Bonn, J., Huber, G., Kluge, H.-J., Otten, E.W.: Z. Phys. A 276, 203 (1976)

[9]     Duke, C., Fischer, H., Kluge, H.-J., Kremmling, H., Kühl, Th., Otten, E.-W.: Phys. Lett. 60 A, 303 (1977)

[10]    Kühl, T., Dabkiewicz, P., Duke, C., Fischer, H., Kluge, H.-J., Kremmling, H., Otten, E.-W.: Phys. Rev. Lett. 39, 180 (1977)

[11]    Dabkiewicz, P., Duke, C., Fischer, H., Kühl, T., Kluge, H.-J., Kremmling, H., Otten, E.-W., Schüssler, H.: J. Phys. Soc. Jap. Suppl. 44, 503 (1978)

[12]    Dabkiewicz, P., Buchinger, F., Fischer, H., Kluge, H.-J., Kremmling, H., Kühl, T., Müller, A.C., Schuessler, H.A.: Phys. Lett. 82B, 199 (1979)

[13]    Otten, E.W.: Proc. Int. School-Seminar on Heavy Ion Physics, Alushta 1983, (Dubna Series D7-83-644, Dubna 1983), p. 158

[14]    Ravn, H.L.: Phys. Reports 54, 201 (1979)

[15]    Arnold, E., Kühl, T., Otten, E.W., von Reisky, L.:   Phys. Lett.
        90A, 399 (1982)

[16]    Buchinger, F., Mueller, A.C., Schinzler, B., Wendt,K., Ekström,
        C., Klempt, W., Neugart, R., Nucl. Instr. and Meth. 202, 159
        (1982)

[17]    Ulm, G., Eberz, J., Huber, G., Lochmann, H., Menges, R., Kir-
        chner, R., Klepper, O., Kühl, T., Larsson, P.O., Marx, D., Mur-
        nick, D., Schardt, D.: Z. Phys. A 321, 395 (1985)

[18]    Mueller, A.C., Buchinger, F., Klempt, W., Otten, E.W., Neugart,
        R., Ekström, C., Heinemeier, J.: Nucl. Phys. A 403, 234 (1983)

[19]    Schneider, F.: Thesis. Berlin 1984

[20]    Dabkiewicz, P.: Thesis. Mainz 1980

[21]    Fulop, G.F., Liu, C.H., Moskowitz, P.A., Redi, O., Stroke, H.H.:
        Phys. Rev. A 9, 593 (1974)

[22]    Redi, O., Stroke, H.H.: Phys. Rev. A 9, 1776 (1974)

[23]    Kleinman, H., Davis, S.P.: J. Opt. Soc. Am. 53, 822 (1963)

[24]    Melissinos, A.C.: Phys. Rev. 115, 126 (1959)

[25]    Melissinos, A.C., Davis, S.P.: Phys. Rev. 115, 130 (1959)

[26]    Hirsch, H.R.: J. Opt. Soc. Am. 51, 1192 (1961)

[27]    Schweitzer, W.G.: J. Opt. Soc. Am. 53, 1055 (1963)

[28]    Crane, J.K., Erbert, G.V., Mostek, S.D., Kerlin, R.C., Paisner,
        J.A.: UCRL-93471 preprint (1985)

[29]    Redi, O., Stroke, H.H.: J. Opt. Soc. Am. 65, 1 (1975)

[30]    Blaise, J., Chantrel, H.: J. Phys. Rad. 18, 193 (1957)

[31]    Heilig, K., Steudel, A.: At. Data Nucl. Data Tables 14, 613 (1974)

[32]    King, W.H.: Isotope Shifts in Atomic Spectra.  New York: Plenum
        Press 1984

[33]    Seltzer, E.C.: Phys. Rev. 188, 1916 (1969)

[34]  Torbohm, G., Fricke, B., Rosén, A.: Phys. Rev. A 31, 2038 (1985)

[35]  Blundell, S.A., Baird, P.E.G., Palmer, C.W.P., Stacey, D.N., Woodgate, G.K., Zimmermann, D.: Z. Phys. A 321, 31 (1985)

[36]  King, W.H.: J. Opt. Soc. Am. 53, 638 (1963)

[37]  Ahmad, S.A., Klempt, W., Ekström, C., Neugart, R., Wendt, K., ISOLDE Collab.: Z. Phys. A 321, 35 (1985)

[38]  Myers, W.D., Schmidt, K.-H.: Nucl. Phys. A 410, 61 (1983)

[39]  McDermott, M.N., Lichten, W.L.: Phys. Rev. 119, 134 (1960)

[40]  Kohler, R.H.: Phys. Rev. 121, 1104 (1961)

[41]  Hahn, A.A., Miller, J.P., Powers, R.J., Zehnder, A., Rushton, A.M., Welsh, R.E., Kunselman, A.R., Roberson, P., Walter, H.K.: Nucl. Phys. A 314, 361 (1979)

[42]  Edelstein, W.A., Pound, R.V.: Phys. Rev. B 11, 985 (1975)

[43]  Kolb, D., Wong, C.Y.: Nucl. Phys. A 245, 205 (1975)

[44]  Krygin, G.B., Mitroshin, V.E.: Sov. J. Nucl. Phys. 41, 193 (1985)

[45]  Heyde, K., van Isacker, P., Waroquier, M., Wood, J.L., Meyer, R.A.: Phys. Rep. 102, 291 (1983)

[46]  Hamilton, J.H., Hansen, P.G., Zganjar, E.F.: Rep. Prog. Phys. 48, 631 (1985)

[47]  Möller, P., Myers, W.D., Swiatecki, W.J., Treiner, J.: Proc. 7th Int. Conf. on Atomic Masses and Fundamental Constants, AMCO-7, Darmstadt-Seeheim 1984, ed.: O. Klepper (THD, Darmstadt 1984), p. 457

[48]  Berdichevsky, D., Tondeur, F.: Z. Phys. A 322, 141 (1985)

[49]  Kumar, K.: Phys. Rev. Lett. 28, 249 (1972)

[50]    Rud, N., Ward, D., Andrews, H.R., Graham, R.L., Geiger, J.S.:
        Phys. Rev. Lett. 31, 1421 (1973)

[51]    Proetel, D., Diamond, R.M., Stephens, F.S.:  Phys. Lett. 48 B,102
        (1974)

[52]    Bockisch, A., Bharuth-Ram, K., Kleinfeld, A.M., Lieb, K.P.:  Z.
        Phys. A 291, 245 (1979)

[53]    Esat, M.T., Kean, D.C., Spear, R.H., Fewell, M.P., Baxter,
        A.M.: Phys. Lett. 72 B, 49 (1977)

[54]    Spear, R.H., Esat, M.T., Fewell, M.P., Kean, D.C., Zabel, T.H.,
        Baxter, A.M., Hinds, S.: Nucl. Phys. A 345, 252 (1980)

[55]    Esat, M.T., Fewell, M.P., Spear, R.H., Zabel, T.H., Baxter,
        A.M., Hinds, S.: Nucl. Phys. A 362, 227 (1981)

[56]    Ahmad, S.A., Ekström, C., Klempt, W., Neugart, R., Otten, E.W.,
        Ulm, G., Wendt, K.: to be published in Nucl. Phys. A

[57]    Wapstra, A.H., Audi, G.: Nucl. Phys. A 432, 55 (1985)

[58]    Thompson, R.C., Anselment, M., Bekk, K., Göring, S., Hanser,
        A., Meisel, G., Rebel, H., Schatz, G., Brown, B.A.: J. Phys. G
        9, 443 (1983)

[59]    Anselment, M., Faubel, W., Göring, S., Hanser, A., Meisel, G.,
        Rebel, H., Schatz, G.: Nucl. Phys. A 451, 471 (1986)

[60]    Andl, A., Bekk, K., Göring, S., Hanser, A., Nowicki, G., Rebel,
        H., Schatz, G., Thompson, R.C.:  Phys. Rev. C 26, 2194 (1982)

[61]    Baxter, A.M., Hinds, S., Spear, R.H., Zabel, T.H., Smith, R.:
        Nucl Phys. A 369, 25 (1981)

[62]    Agarwal, Y.K., Günther, C., Hardt, K., Schüler, P., Stachel, J.,
        Wollersheim, H.J., Emling, H., Grosse, E., Kulessa, R., Spreng,
        W.:  Z. Phys. A320, 295 (1985)

[63]    Möller, P., Nix, J.R.: At. Data  Nucl. Data Tables 26, 165 (1981)

[64]  Gerhardt, H., Matthias, E., Rinneberg, H., Schneider, F., Timmermann, A., Wenz, R., West, P.J.: Z. Phys. A 292, 7 (1979)

[65]  Faessler, A., Götz, U., Slavov, B., Ledergerber, T.: Phys. Lett. 39 B, 579 (1972)

[66]  Cailliau, M., Letessier, J., Flocard, H., Quentin, P.: Phys. Lett. 46 B, 11 (1973)

[67]  Dickmann, F., Dietrich, K.: Z. Phys. 263, 211 (1973)

[68]  Nilsson, S.G., Nix, J.R., Möller, P., Ragnarsson, I.: Nucl. Phys. A 222, 221 (1974)

[69]  Frauendorf, S., Pashkevich, V.V.: Phys. Lett. 55B, 365 (1975)

[70]  Bengtsson, R., Möller,P., Nix, J.R., Zhang, J.: Phys. Scripta 29, 402 (1984)

[71]  Möller, P., Nix, J.R.: Nucl. Phys. A 361, 117 (1981)

[72]  Ma, W.C., Ramayya, A.V., Hamilton, J.H., Robinson, S.J., Barclay, M.E., Zhao, K., Cole, J.D., Zganjar, E.F., Spejewski, E.H.: Phys. Lett. 139B, 276 (1984)

[73]  Ragnarsson, I.: in "Future Directions in Studies of Nuclei far from Stability", Proc. Int. Symp., Nashville 1979, eds.: Hamilton, J.H., Spejewski, E.H., Bingham, C.R., Zganjar, E.F. (North-Holland Publ. Comp., Amsterdam 1980), p. 367

[74]  Praharaj, C.R., Khadkikar, S.B.: J. Phys. G 6, 241 (1980)

[75]  Barfield, A.F., Barrett, B.R., Sage, K.A., Duval, P.D.: Z. Phys. A 311, 205 (1983)

[76]  Barfield, A.F., Barrett, B.R.: Phys. Lett. 149B, 277 (1984)

[77]  Barfield, A.F.: Private communication (1985)

[78]  Reehal, B.S., Sorensen, R.A.: Nucl. Phys. A 161, 385 (1971)

[79]    Stroke, H.H., Proetel, D., Kluge, H.J.:    Phys. Lett. 82 B, 204
        (1979)

[80]    Talmi, I.: Nucl. Phys. A 423, 189 (1984)

[81]    Zawischa, D.: Phys. Lett. 155B, 309 (1985)

[82]    Ekström, C., Wannberg, G., Shishodia, Y.S.:    Hyperfine Interact.
        1, 437 (1976)

[83]    Ekström, C.: 4th Int. Conf. on Nuclei far from Stability, Helsingor
        1981, eds.: Hansen, P.G., Nilssons, O.B. (CERN, Report 81-09,
        Geneva 1981), p. 12

[84]    Volmyanskii, E.I., Dubro, V.G.: Izvestiya Akademii Nauk SSSR,
        Ser. Fiz. 41, no. 6, 1249 (1977)

[85]    Löbner, K.E.G., Vetter, M., Hönig, V.:    Nucl. Data Tables A 7,
        495 (1970)

[86]    Proetel, D., Benson, Jr., D., Gizon, A., Gizon, J., Maier, M. R.,
        Diamond, R.M., Stephens, F.S.: Nucl. Phys. A 226, 237 (1974)

[87]    Faessler, A.: Hyperfine Interact. 9, 3 (1981)

[88]    Wilson, M.: Phys. Rev. 176, 58 (1968)

[89]    Guern, Y., Bideau-Mehu, A., Abjean, R., Johannin-Gilles, A.:
        Phys. Scripta 14, 273 (1977)

[90]    Kopfermann, H.: Nuclear Moments. New York: Academic Press Inc.
        1958

[91]    Major, F.G., Werth, G.: Phys. Rev. Lett. 30, 1155 (1973)

[92]    Lederer, C.M., Shirley, V.S.: Table of Isotopes.    7th Edn. New
        York: Wiley 1978

[93]    Rosenberg, H.J., Stroke, H.H.: Phys. Rev. A 5, 1992 (1972)

[94]    Lee, P.L., Boehm, F., Hahn, A.A.: Phys. Rev. C 17, 1859 (1978)

[95]  Bauche, J., Hühnermann, H., Stacey, D.N., Stacey, V., Wilson, M.: Z. Phys. A 320, 157 (1985)

[96]  Bauche, J.: Comm. At. Mol. Phys. 10, 57 (1981)

[97]  Blundell, S.A., Baird, P.E.G., Botham, C.P., Palmer, C.W.P., Stacey, D.N., Woodgate, G.K.: J. Phys. B 17, 53 (1984)

[98]  Murakawa, K.: J. Phys. Soc. Jap. 14, 1624 (1959)

[99]  Murakawa, K.: J. Phys. Soc. Jap. 20, 1094 (1965)

[100]  Lurio, A.: Phys. Rev. 142, 46 (1966)

[101]  Kluge, H.-J., Sauter, H.: Z. Phys. 270, 295 (1974)

[102]  Schwartz, C.: Phys. Rev. 105, 173 (1957)

[103]  Sobel'man, I.I.: Introduction to the Theory of Atomic Spectra. Oxford: Pergamon Press 1972

[104]  Kluge, H.-J.: Thesis. Heidelberg 1970

[105]  data from: Swagel, M.W., Lurio, A.: Phys. Rev. 169, 114 (1968), Reimann, R.J., McDermott, M.N.: Phys. Rev. C7, 2065 (1973) and Ref. [39]

[106]  Olsson, G., Salomonson, S.: Z. Phys. A 307, 99 (1982)

[107]  Lindgren, I., Rosen, A.: Case Studies in Atomic Physics 4, 93 (1975)

[108]  Wendt, K., Ahmad, S.A., Klempt, W., Neugart, R., Otten, E.W., Stroke, H.H.: submitted to Z. Phys. D

[109]  Sternheimer, R.M.: Private communication (1982) and Phys. Rev. A6, 1702 (1972) and references therein

Fig. 1: Part of the energy level scheme of Hg I, includingd the ground state of the charge exchange partner Na relative to the ionization limit of Hg. The almost resonant exchange condition to the $^3P_2$ state is evident. The $\lambda$ = 546.1 nm transition was studied by collinear laser spectroscopy.

Fig. 2: Fluorescence signals as a function of the acceleration voltage for the case of $^{182}$Hg, $^{184}$Hg, and $^{198}$Hg. The integration time per channel was 1 s, 0.4 s, and 0.1 s, respectively.

Fig. 3: King-plot of the IS in the 546 nm line versus those in the 254 nm line. The common reference isotope is $^{198}$Hg.

Fig. 4: Changes of mean square charge radii $\delta\langle r^2\rangle$ in the isotopic chain $^{181-206}$Hg as a function of the mass number A, with $^{198}$Hg taken as a reference. The almost straight solid line correponds to the change in $\delta\langle r^2\rangle$ due to the pure volume effect at constant deformation as given by the droplet model. The data points for the ground states are connected by a line to guide the eye.

Fig. 5: Plot of the differences of nuclear mean square charge radii between even isotopes for Hg (Z=80) and Pb (Z=82) [58], [59]. The solid curves are drawn to guide the eye. The almost horizontal dashed line shows the prediction of the spherical droplet model.

Fig. 6: Odd-even staggering parameter γ of the nuclear mean square charge radii of the ground states (upper part) and of the I = 13/2 isomers (lower part) of Hg I isotopes. The γ parameters of nuclei with identical nuclear spins are connected with a solid line to guide the eye.

Table 1: Compilation of isotope shift data $\delta v^{198,A}$ in the transitions $6s^2\ ^1S_0$ - $6s6p\ ^3P_1$ ($\lambda$ = 253.7 nm) and $6s6p\ ^3P_2$ - $6s7s\ ^3S_1$ ($\lambda$ = 546.1 nm) of Hg I and of the differences in nuclear mean square charge radii evaluated from these data. Results for the nuclear ground states and I = 13/2 isomers are given. The errors listed for $\delta\langle r^2\rangle$ are purely experimental. An additional scaling error stems from the uncertainty of the F-factor (7%) and the SMS. The scaling uncertainty due to the SMS is 0.4% except for the strongly deformed isotopes $^{181}$Hg, $^{183}$Hg, $^{185}$Hg, where it is about 4% due to the relatively small field shift of these isotopes. Rms deformation parameters $\langle\beta_2^2\rangle^{1/2}$ are listed in column 5 and 6. $\beta_{IS}$ was fixed to $\beta_{B(E2)}$ at $^{198}$Hg. The first of the brackets behind the model dependent parameter $\beta_{IS}$ gives the pure experimental error, the second indicates the systematic one which stems from the scaling uncertainty of the F-factor and the SMS.

| A | $\delta\nu^{198,A}$ (MHz) | | $\delta\langle r^2\rangle^{198,A}$ | $\langle\beta_2{}^2\rangle^{1/2}$ | |
|---|---|---|---|---|---|
| | 253.7 nm | 546.1 nm | (fm²) | from IS | from B(E2) |
| 181 | 5560(200)[a] | - | -0.0953(33) | 0.283(2){2} | - |
| 182 | - | -5890(17)* | -0.6384(20) | 0.169(2){12} | - |
| 183 | 3310(100)[a] | - | -0.0527(16) | 0.273(2){1} | - |
| 184 | 27720( 90)[b,c] | -4932(14)* | -0.5337(13) | 0.169(2){11} | 0.16(2)[u] |
| 185 | 3710( 30)[a,c] | - | -0.0622 (6) | 0.254(2){1} | - |
| 185m | 27770(110)[c,d] | - | -0.5357(22) | 0.155(2){11} | - |
| 186 | 24060( 70)[b,c] | -4285(11)* | -0.4643(10) | 0.160(2){10} | 0.13(1)[v] |
| 187 | 22420(200)[a,c] | - | -0.4324(40) | 0.154(2){9} | - |
| 187m | 23970(120)[d] | - | -0.4630(24) | 0.146(2){10} | - |
| 188 | 20420( 80)[b,c] | -3629(10)* | -0.3944(10) | 0.150(2){9} | - |
| 189 | 19620(120)[a,c] | - | -0.3793(24) | 0.139(2){9} | - |
| 189m | 20050( 60)[d] | - | -0.3877(13) | 0.137(2){10} | - |
| 190 | 16560( 80)[c,e] | -2925( 7)* | -0.3188 (8) | 0.142(2){8} | - |
| 191 | 15710( 70)[a,c] | - | -0.3041(15) | 0.130(1){8} | - |
| 191m | 15690( 60)[d] | - | -0.3037(13) | 0.130(1){8} | - |
| 192 | 12810(230)[a,f,g] | -2203( 7)* | -0.2405(14) | 0.133(2){6} | - |
| 193 | 12060(410)[g,i] | - | -0.2340(80) | 0.117(4){6} | - |
| 193m | 11150(120)[d,f,g,j] | - | -0.2160(24) | 0.124(2){5} | - |
| 194 | 8480(180)[f,k] | -1471( 5)* | -0.1607 (7) | 0.125(2){4} | - |
| 195 | 6370(110)[f,g,k] | - | -0.1234(22) | 0.119(2){3} | - |
| 195m | 6780(110)[d,f,g,k] | - | -0.1315(22) | 0.116(2){4} | - |
| 196 | 4110(120)[l] | -740 (4)*<br>-740.0(1.5)[s] | -0.0809 (3) | 0.116(2){2} | 0.114(1)[w] |
| 197 | 2730(150)[l] | - | -0.0532(30) | 0.106(2){2} | - |
| 197m | 2200( 80)[d,m,n] | - | -0.0427(16) | 0.110(2){1} | - |
| 198 | 0 | 0 | 0 | 0.106(1) | 0.106(1)[w,x] |

| 199 | $-651.7(5.4)^{o,p}$ | 90 (30)$^t$ | 0.0119 (2) | 0.088(1){1} | - |
|---|---|---|---|---|---|
| 199m | $-3190$ (150)$^d$ | - | 0.0623(30) | 0.110(2){1} | - |
| 200 | $-4806.9(3.9)^{o,p}$ | 845.5(1.5)$^{s,t}$ | 0.0935 (2) | 0.101(1){3} | 0.098(1)$^{w,y}$ |
| 201 | $-6414.1(5.7)^{o,p}$ | 1110 (30)$^t$ | 0.1245 (2) | 0.091(1){4} | - |
| 202 | $-10102.4(4.2)^{o,p}$ | 1776.8(2.1)$^{s,t}$ | 0.1970 (2) | 0.100(1){6} | 0.082(1)$^{w,y}$ |
| 203 | $-11750$ (180)$^q$ | - | 0.2288(36) | 0.090(3){7} | - |
| 204 | $-15311.6(9.9)^{o,p}$ | 2690.7(2.6)$^{s,t}$ | 0.2988 (3) | 0.098(2){9} | 0.068(1)$^{w,z}$ |
| 205 | $-17090$ (100)$^a$ | - | 0.3333(20) | 0.089(2){10} | - |
| 206 | $-20420$ ( 80)$^{c,r}$ | - | 0.3987(17) | 0.095(2){12} | - |

* This work: Collinear laser spectroscopy.

a Reference [8]

b Reference [10]

c Reference [20]

d Reference [12]

e Reference [9]

f Reference [2]

g Reference [3]

i Reference [21]

j Reference [22]

k Reference [23]

l Reference [24]

m Reference [25]

n Reference [26]

o Reference [27]

p Reference [28]

q Reference [29]

[r] Reference [11]

[s] Reference [19]

[t] Reference [30]

[u] Reference [50]

[v] Reference [51]

[w] Reference [52]

[x] Reference [53]

[y] Reference [54]

[z] Reference [55]

Table 2: Hyperfine interaction constants of the Hg I 6s6p $^3P_1$ state of neu-
tron deficient Hg isotopes measured with pulsed lasers on atoms confined in
resonance cells. The values of the magnetic dipole moments $\mu$ are corrected
for diamagnetism.

| A | I | A (GHz) | B (GHz) | $\mu$ (n.m.) |
|---|---|---------|---------|--------------|
| 185 | 1/2 | 14.96(7)[a] | - | 0.509(4)[b] |
| 187 | 3/2 | -5.83(4)[a] | 0.54(13)[a] | -0.594(4)[c] |
| 189 | 3/2 | -5.81(6)[a] | 0.55(20)[a] | -0.6086(8)[c] |
| 191 | 3/2 | -6.02(4)[a] | 0.58(13)[a] | -0.618(11)[c] |
| 185m | 13/2 | -2.305(19) | -0.14(23) | -1.017(9)[d] |

[a] Weighted mean of RADOP-data [8] and laser spectroscopic results [20].

[b] Weighted mean of direct RADOP-results [8] and a magnetic moment deter-
mined from the A-factor with the help of the ratio $A(^{195}Hg)/\mu(^{195}Hg)$ with
an estimated error of $1\times10^{-2}$ accounting for the hyperfine anomaly.

[c] Same procedure as in [b] with the ratio $A(^{201}Hg)/\mu(^{201}Hg)$.

[d] From the A-factor with the help of the known ratio
$A(^{193m}Hg)/\mu(^{193m}Hg)$. An error of $1\times10^{-3}$ accounting for the hyperfine
anomaly is included.

Table 3: Compilation of spectroscopic quadrupole moments $Q_s$ of the nuclear ground states and $I = 13/2$ isomers of Hg isotopes. The moments are evaluated taking as reference the values $B(6s6p\ ^3P_1) = -0.280107(5)$ GHz [40] and $Q_s = 0.372(40)$ b for $^{201}$Hg. The B factors used for the evaluation of $Q_s$ are listed in Table 2 of this work, in Table 3 of Ref. [8], and in Table 1 of Ref. [12]. The errors listed for $Q_s$ include the scaling uncertainty from the reference value.

| A | 185m | 187 | 187m | 189 | 189m | 191 | 191m |
|---|---|---|---|---|---|---|---|
| $Q_s$ (b) | 0.19(33) | -0.72(25) | 0.45(33) | -0.73(35) | 0.64(26) | -0.77(25) | 0.62(25) |

| A | 193 | 193m | 195m | 197m | 199m | 201 | 203 |
|---|---|---|---|---|---|---|---|
| $Q_s$ (b) | -0.70(38) | 0.885(97) | 1.04(11) | 1.20(14) | 1.14(45) | 0.372(40) | 0.331(36) |

Table A1: Comparison of the electronic factor $F_{254}$ for the transition $6s^2\ {}^1S_0$ - $6s6p\ {}^3P_1$ ($\lambda$ = 253.7 nm) in Hg I.

| $F_{254}$ (GHz/fm²) | Method |
| --- | --- |
| -55.36 | ab initio relativistic MCDF calculation [34] |
| -60.3(6.0) | semi-empirical calculation |
| -55.1(3.1) | electronic X-ray data [94] |
| -52.1(1.0) | muonic X-ray data [41] |

G. Huber

R. Neugart

E.-W. Otten

K. Wendt

Institut für Physik

Universität Mainz

Postfach 3980

D-6500 Mainz

Federal Republic of Germany


W. Klempt

H.-J. Kluge

G. Ulm

CERN

CH-1211 Geneva 23

Switzerland


S.K. Bhattacherjee

Tata Institute of Fundamental Research

Homi Bhabha Road

Bombay 400 005

India

P. Dabkiewicz

Technische Universität Hamburg-Harburg

Arbeitsbereich Optik und Meßtechnik

Harburger Schloßstr. 20

D-2100 Hamburg 90

Federal Republic of Germany


T. Kühl

Gesellschaft für Schwerionenforschung mbH

Postfach 110541

D-6100 Darmstadt 11

Federal Republic of Germany


H. Lochmann

W.C. Heraeus GmbH

Heraeusstr. 12 - 14

D-6450 Hanau 1

Federal Republic of Germany


S.A. Ahmad

Spectroscopy Division

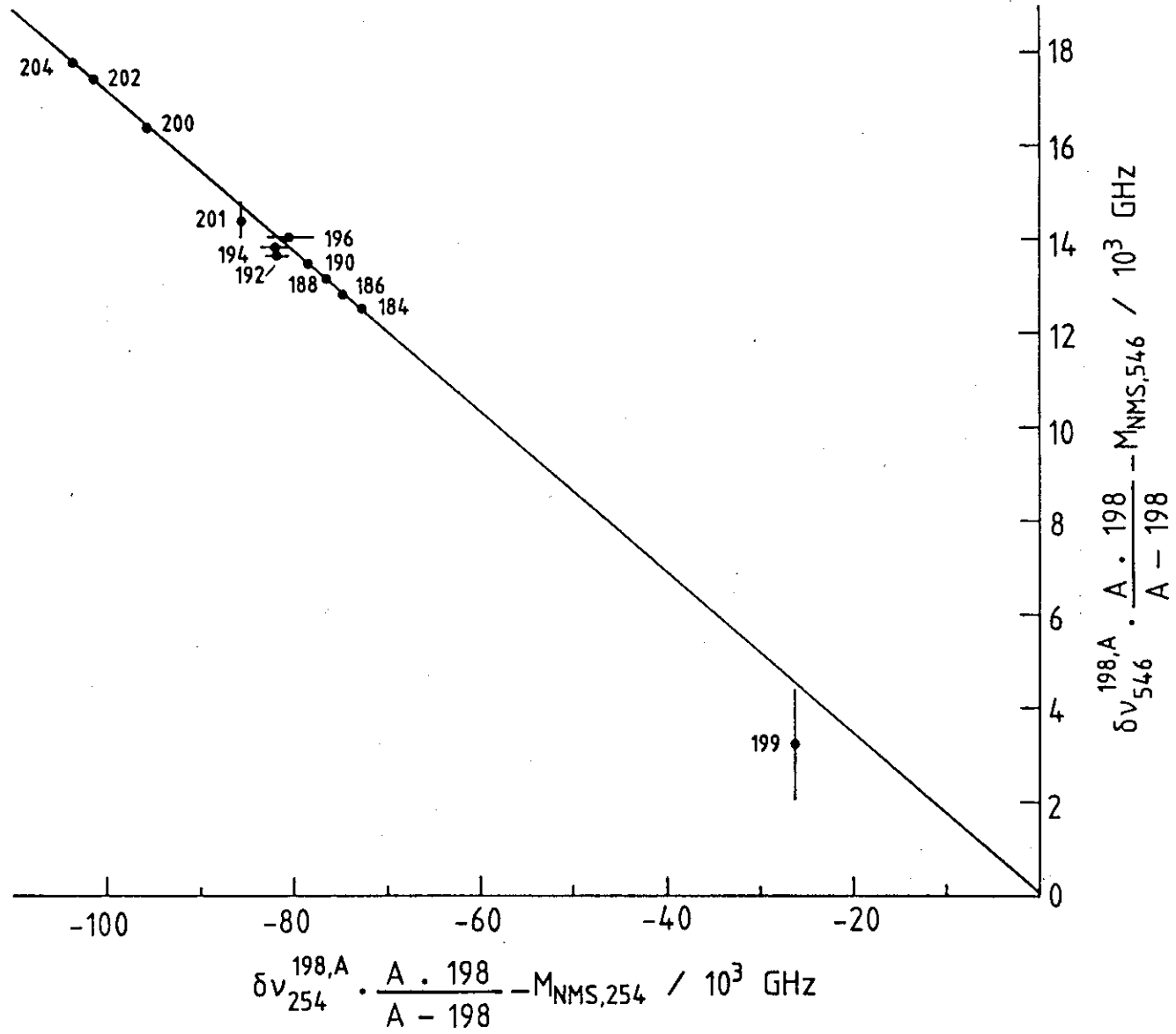Bhabha Atomic Research Centre

Trombay

Bombay 400 085

India
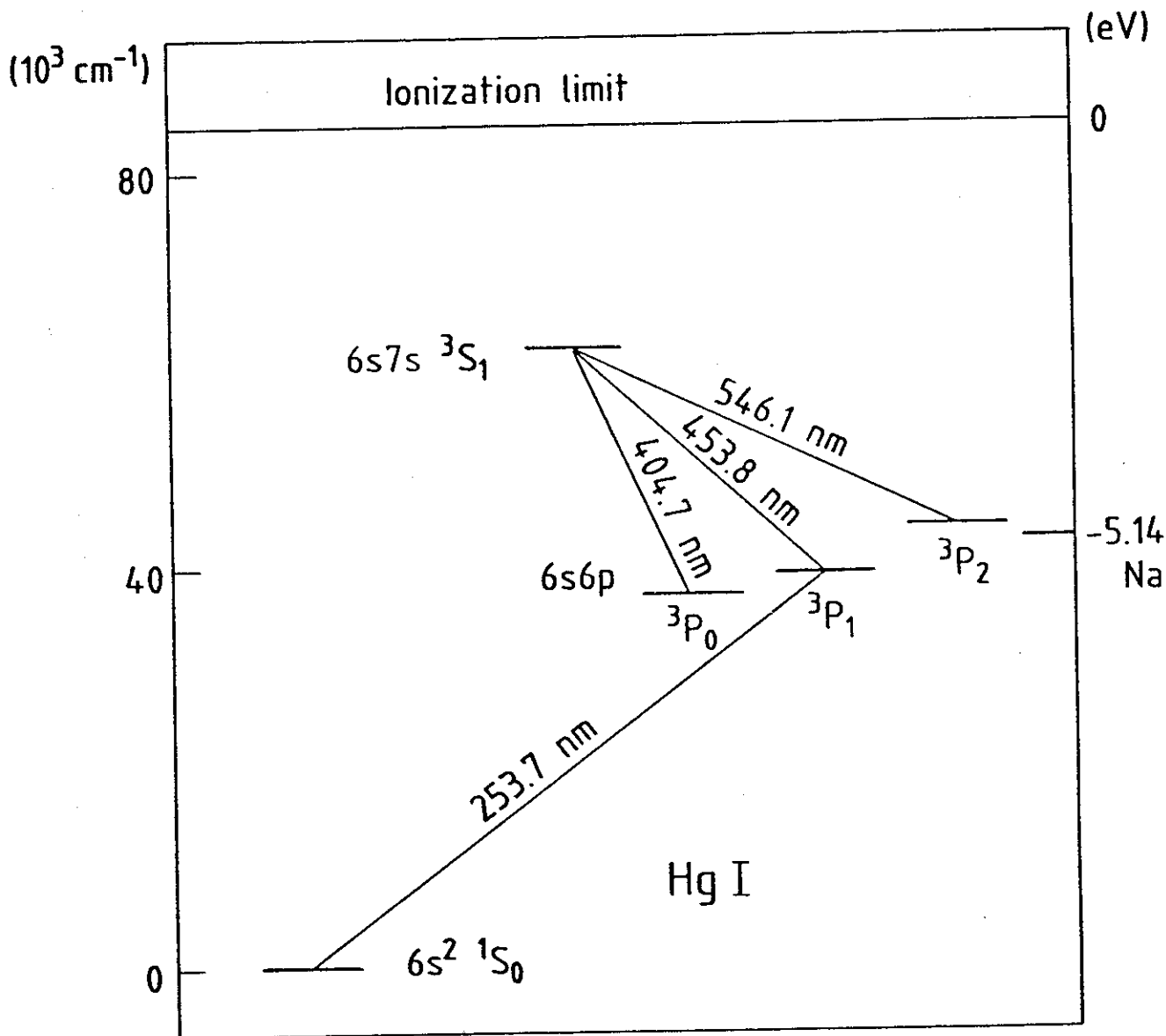
Fig. 1

Fig. 2

Fig. 3

Fig. 4

Fig. 5

Fig. 6